

SNOwGLoBES: SuperNova Observatories with GLoBES: DRAFT

Alex Beck¹, Farzan Beroz¹, Rachel Carr², Huaiyu Duan³,
Alex Friedland⁴, Nicolas Kaiser^{5,1}, Jim Kneller⁶, Alexander Moss¹,
Diane Reitzner⁷, Kate Scholberg^{1*}, David Webber⁸, Roger Wendell¹

¹ Department of Physics, Duke University, Durham, NC 27705

² Department of Physics, Columbia University, New York, NY 10027

³ Department of Physics, University of New Mexico, Albuquerque, NM, 87131

⁴ Los Alamos National Laboratory, Los Alamos, NM, 87545

⁵ Department of Physics, Karlsruhe Institute of Technology, Germany

⁶ Department of Physics, North Carolina State University, Raleigh, NC, 27695

⁷ Fermilab, Batavia, IL, 60510-5011

⁸ Department of Physics, University of Wisconsin, Madison, WI, 53706-1390

* `schol@phy.duke.edu`

Version 1.1 August 31, 2014

Abstract

This document describes public software for computing interaction rates and distributions of observed quantities for supernova burst neutrinos in common detector materials. The intent is to provide a very simple and fast code and data package which can be used for tests of observability of physics signatures in current and future detectors, and for evaluation of relative sensitivities of different detector configurations. The event estimates are made using available cross-sections and parameterized detector responses. Water, argon, scintillator and lead-based configurations are included. The package makes use of GLoBES front-end software. SNOwGLoBES is not intended to replace full detector simulations; however output should be useful for many types of studies. This document serves as a user's manual and provides references for the data files used.

1 Introduction

A stellar core collapse in the Milky Way or nearby will produce an enormous burst of neutrinos observable in terrestrial detectors. Such a burst will carry tremendous information

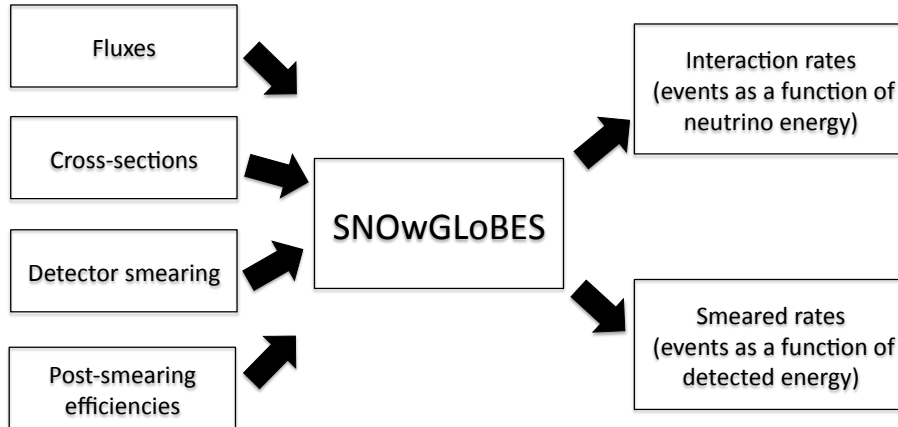


Figure 1: SNOwGLoBES data flow.

about both astrophysics and particle physics: see [1] for recent reviews of physics reach and [2] for an overview of detection technology.

To enable fast, informative studies of the physics potential of the detection of supernova neutrinos, we have developed a simple software and database package to compute expected event rates by folding input fluxes with cross-sections and detector parameters. The output is in the form of interaction rates for each channel as a function of neutrino energy, and “smeared” rates as a function of detected energy for each channel (*i.e.* the spectrum that actually be observed in a detector). For this study we have chosen to do the event rate computation by using parameterized detector responses, making use of the GLoBES software [3, 4]. We employ only the front-end rate engine part of GLoBES, and not the oscillation sensitivity part. GLoBES takes as input fluxes, cross sections, “smearing matrices” and post-smearing efficiencies. The smearing matrices incorporate both interaction product spectra and detector response. Fig. 1 gives a schematic overview of the approach.

Although with this approach, information is lost with respect to a full event-by-event simulation using a neutrino interaction generator and detector simulation (correlations between energy and angle are lost, for example), nevertheless it offers a fast, simple method useful for many studies.

The software should enable studies from differing points of view, by allowing modification of the different kinds of input. For example:

- Using the standard cross-sections and detector parameters, one can study whether specific physics signatures in the fluxes are observable with different detector configurations.
- Experimentalists can optimize detector configurations by using standard cross-sections and the sample fluxes, and modifying the smearing, efficiency and background files according to different configurations (for example, different PMT coverages in a water

Cherenkov configuration). An early version of SNOwGLOBES was used in this way for the work described in reference [5].

- One could also study systematic errors due to cross-section uncertainties (for example) by comparing event rates computed using cross-sections from different models or with modifications according to estimated uncertainties.

Currently, time-dependent fluxes are not supported explicitly; however time dependence can be straightforwardly handled by providing multiple files with fluxes divided into different time bins.

Users should note that SNOwGLOBES *does not employ the oscillation probability and parameter sensitivity computation functionality of GLOBES at all*. Although SNOwGLOBES can be helpful for studies of neutrino oscillation by, for example, enabling the comparison of expected oscillated and non-oscillated fluxes (for oscillation in supernova or Earth), the user must compute the oscillation probabilities modulating the flux and evaluate sensitivities separately. SNOwGLOBES is simply an event rate calculator.

2 Software Overview

2.1 Dependencies

GLOBES [4] version 3.0.15 or later and its dependencies (3.1.6 for Mac) must be installed, and the environment variable `GLB_DIR` must be set to the GLOBES installation directory. `Perl` is also required, and `Root` [6] is required for the sample plotting scripts.

2.2 Download and Installation Instructions

The package is available from the Duke `svn` repository.

- Download version 1.1 with
`svn co http://svn.phy.duke.edu/repos/neutrino/snowglobes/tags/snowglobes-1.1`
with `userid` and `password guest/guest`.
- Set the environment variable `SNOWGLOBES` to the installation directory.
- Set the environment variable `GLB_DIR` to where you have installed GLOBES.
- Go to `SNOWGLOBES/src` and type `make`, then `make install`.
- That's it. Run the scripts from the `SNOWGLOBES` directory.

2.3 Files

The `SNOWGLOBES` package has data files organized into several subdirectories:

- `$$SNOWGLOBES/backgrounds` contains the additive background files, labeled by detector configuration.
- `$$SNOWGLOBES/bin` contains the `GLOBES` executable run by the main script.
- `$$SNOWGLOBES/channels` contains the files listing relevant channels for each detector type.
- `$$SNOWGLOBES/doc` contains documentation for installation and running, and references for the included data files.
- `$$SNOWGLOBES/effic` contains the post-smearing efficiency files in `GLOBES` format, labeled by interaction type and detector configuration.
- `$$SNOWGLOBES/fluxes` contains the flux files in `GLOBES` format, labeled by flux name.
- `$$SNOWGLOBES/glb` contains some template files required for building the `GLOBES` file.
- `$$SNOWGLOBES/out` contains output files generated by `SNOWGLOBES`, labeled by interaction type and detector configuration, for both interaction rates and smeared rates.
- `$$SNOWGLOBES/plots` contains some sample Root plotting scripts.
- `$$SNOWGLOBES/smear` contains the smearing matrix files in `GLOBES` format, labeled by interaction type and detector configuration.
- `$$SNOWGLOBES/xscns` contains the cross-section files in `GLOBES` format, labeled by interaction channel.

2.4 Running the Software

The primary tool is a script called `supernova.pl`. This takes three arguments: the flux file label, the channel file label, and the experiment configuration name.

The channel file gives a list of channels for which `SNOWGLOBES` should compute event rates, and the appropriate target weighting factor for each of these channels. Example channels files can be found in the `$$SNOWGLOBES/channels` subdirectory. The user can modify these to select desired channels. See section 6 for information about how to add new channels.

For example, to compute event rates for HALO2 for “Livermore” flux and the interaction channels in `$$SNOWGLOBES/channels/channels_lead.dat`, do

```
./supernova.pl livermore lead halo2
```

Output goes to the `$$SNOWGLOBES/out` subdirectory, into spectrum files named by flux, channel, and experiment configuration. Output text files are generated both for interaction rates (as a function of neutrino energy), and for rates smeared by detector response, as a

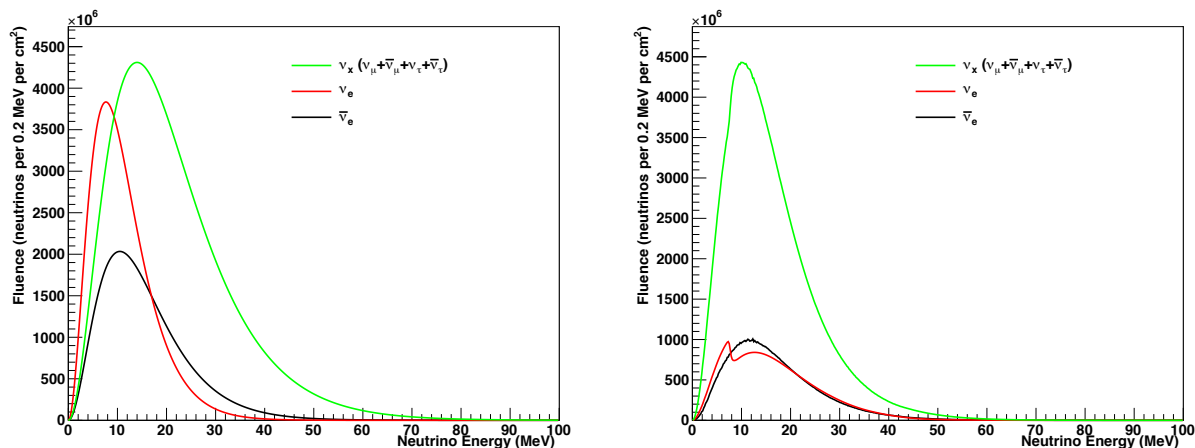


Figure 2: Left: “Livermore” fluence, for different flavor components, from reference [7], assuming Fermi-Dirac spectra with the average energies indicated as a function of time and zero chemical potential, and integrated from $t = 0$ to $t = 14$ seconds. Right: “GVKM” fluence, integrated over 10 seconds.

function of detected energy (the latter are labeled “_smearred”). The first column of the output file is energy (either neutrino energy or, for smeared output, detected energy), and the second column is event rate in that energy bin (events per 0.5 MeV).

Files for which event rates are not weighted by target weighting factor (see section 6.2) are labeled “_unweighted”. As of SNOwGLoBES version 1.1, the `supernova.pl` script applies the weighting factors to create the output files.

`make_event_table.pl` is a sample script to return integrated rates for each channel. It takes the same arguments as `supernova.pl`; add an additional argument “1” if a table of non-smeared rates is desired. The plotting scripts in the `$SNOWGLOBES/plots` directory also give examples of plotting output rates.

3 Supernova Neutrino Fluxes

Supernova neutrino fluxes must be provided in GLoBES file format. Two example fluxes are provided with the package: the “Livermore” flux [7], and the “GVKM” flux [8]. Strictly speaking, these are not fluxes but fluences: they are integrated over the time of the burst. The spectra for the flavor components of these two example fluences are plotted in Fig. 2. We will include more fluxes, and flux generation tools, in the future.

4 Neutrino Interaction Cross-sections

We provide cross-sections relevant for four detector materials relevant for current and near-future detectors: water, scintillator, argon and lead. Distributions of interaction products

are taken into account in the “smearing” matrices (see Section 5). We expect future upgrades of SNOwGLOBES to incorporate more channels and more materials.

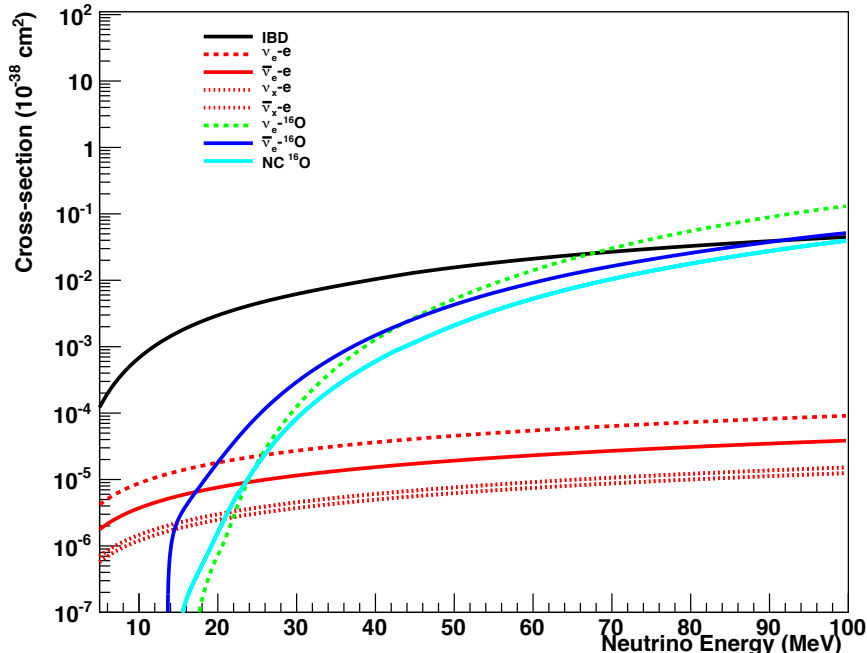


Figure 3: Cross sections for relevant processes in water.

4.1 Inverse Beta Decay

Inverse beta decay $\bar{\nu}_e + p \rightarrow e^+ + n$ (IBD) is dominant for detectors with free protons, such as water and scintillator. We use the cross-section from reference [9], plotted in Fig. 3.

4.2 Neutrino-Electron Elastic Scattering

The cross-sections for elastic scattering (ES) of neutrinos on electrons $\nu_{e,x} + e^- \rightarrow \nu_{e,x} + e^-$ (both NC and CC) are known to better than percent level [10]. These cross-sections are plotted in Fig. 3. The electron ES interaction is relevant for all targets, although the scattered electrons may not be observable for some detector configurations (*e.g.* HALO).

4.3 Interactions with Oxygen

Interactions on oxygen include the CC interactions $\nu_e + {}^{16}\text{O} \rightarrow e^- + {}^{16}\text{F}$, $\bar{\nu}_e + {}^{16}\text{O} \rightarrow e^+ + {}^{16}\text{N}$. These interactions have diverse final states, including ejected nucleons and deexcitation gammas in addition to the produced lepton. For the NC interaction with ${}^{16}\text{O}$, $\nu_x + {}^{16}\text{O} \rightarrow$

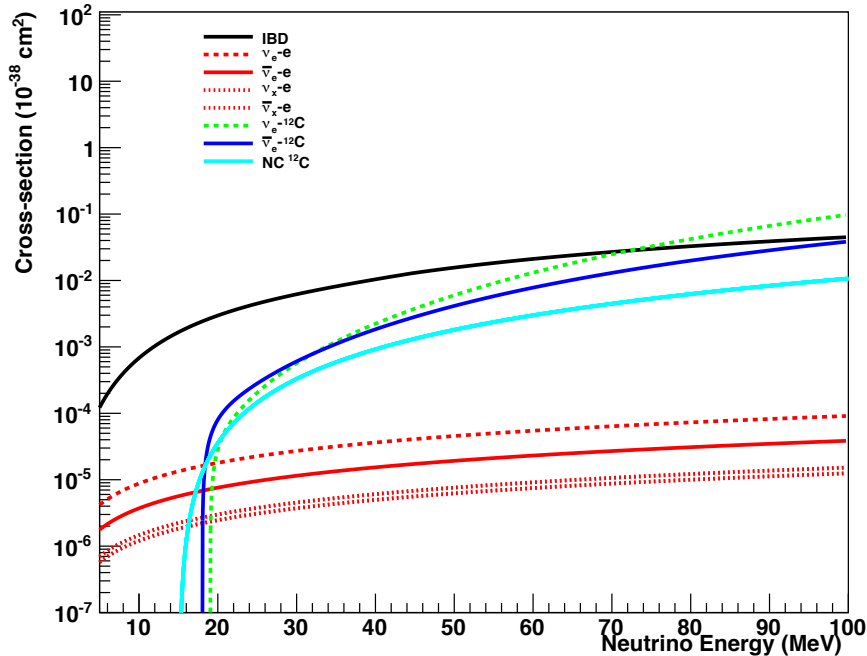


Figure 4: Cross sections for relevant processes in scintillator.

$\nu_x + {}^{16}\text{O}^*$, de-excitation gammas are in principle observable. We use cross-sections from reference [11]. Oxygen cross-sections are plotted in Fig. 3.

4.4 Interactions with Carbon

Electron flavor neutrinos will interact with carbon nuclei via the CC interactions $\nu_e + {}^{12}\text{C} \rightarrow {}^{12}\text{N} + e^-$ and $\bar{\nu}_e + {}^{12}\text{C} \rightarrow {}^{12}\text{B} + e^+$. An NC excitation interaction, $\nu_x + {}^{12}\text{C} \rightarrow \nu_x + {}^{12}\text{C}^*$ also takes place; this interaction results in a 15.5 MeV de-excitation γ -ray which can be used to tag this interaction. We use cross-sections from reference [12] for the CC interactions and the measurement from reference [13] for the NC cross-section. Carbon cross-sections are plotted in Fig. 4.

4.5 Interactions with Argon

We include the CC interactions $\nu_e + {}^{40}\text{Ar} \rightarrow e^- + {}^{40}\text{K}^*$, and $\bar{\nu}_e + {}^{40}\text{Ar} \rightarrow e^+ + {}^{40}\text{Cl}^*$. The cross sections for interactions in argon, from references [14, 15], are shown in Fig. 5. The uncertainties for the recent calculations are at around the 10-20% level. We do not include the NC $\nu_x + {}^{40}\text{Ar} \rightarrow \nu_x + {}^{40}\text{Ar}^*$ channel at this time due to lack of information in the literature about resulting observable products.

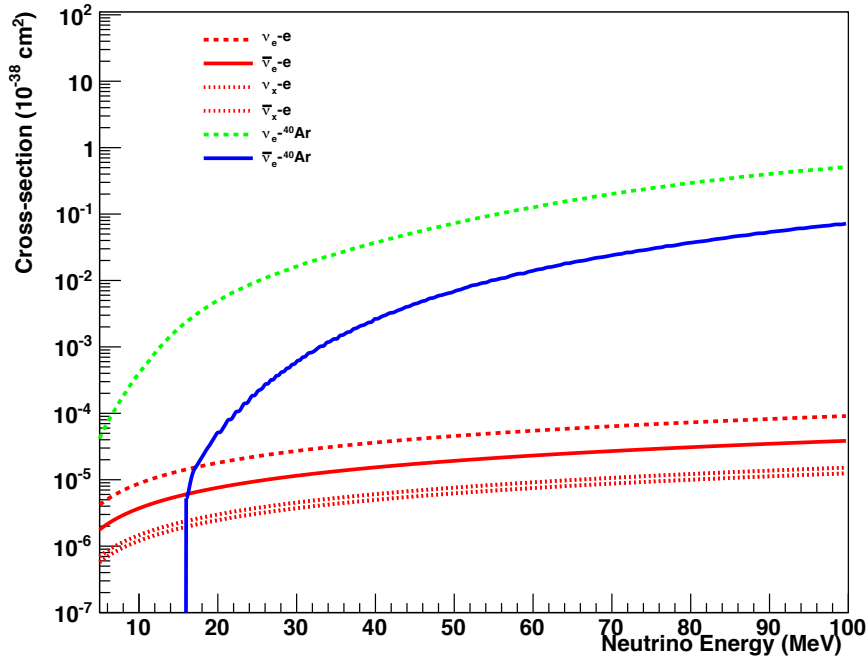


Figure 5: Cross sections for relevant processes in liquid argon.

4.6 Interactions with Lead

For lead, we include CC and NC cross-sections for both single and double neutron ejection channels for: $\nu_e + {}^{208}\text{Pb} \rightarrow e^- + {}^{208}\text{Bi}^*$, $\nu_x + {}^{208}\text{Pb} \rightarrow \nu_x + {}^{208}\text{Pb}^*$, $\bar{\nu}_x + {}^{208}\text{Pb} \rightarrow \bar{\nu}_x + {}^{208}\text{Pb}^*$.

We use cross-sections from [16]. Lead cross-sections are plotted in Fig. 6. Uncertainties on lead cross-sections are evaluated in [17].

5 Detector Response Parameters

The smearing matrices provided are also in GLOBES format. The spectral distributions of interaction products and the detector response are handled simultaneously by this matrix: each column of the matrix represents the detector response for a given monochromatic incoming neutrino energy. The GLOBES-formatted efficiency files give the detector efficiency as a function of detected energy for a given channel and detector configuration.

For some of the provided smearing files, published information was used; for others, the LBNE simulation package has been used. Some estimates may be rather optimistic, as we tend to use optimistic smearing when little detailed information is available. Users may also provide their own smearing matrices and efficiency information. We will update smearing files as knowledge of expected detector responses improves.

Background is also handled: the user can provide a file of background as a function of energy to be smeared by the indicated detector response. This is handled by creating a “fake”

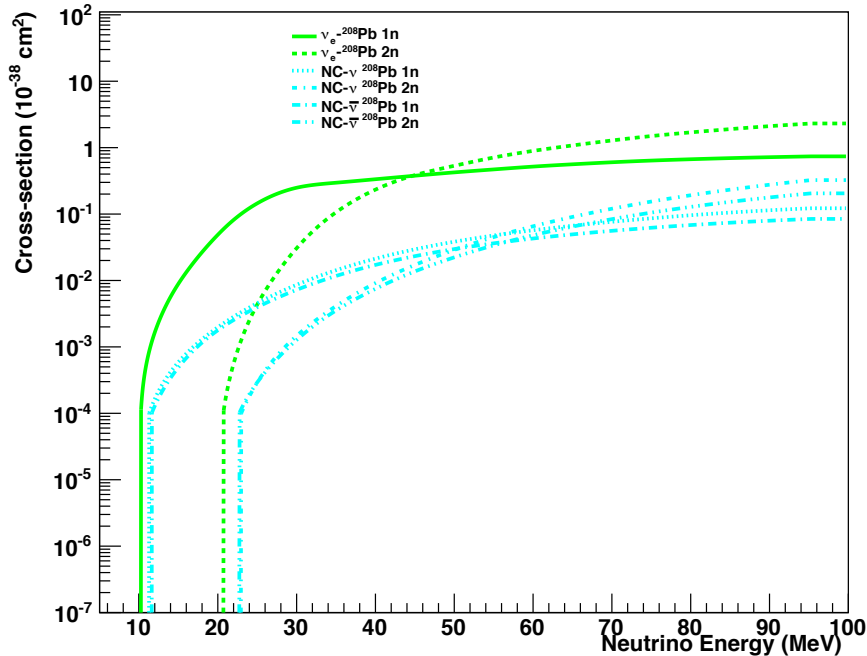


Figure 6: Cross sections for relevant processes in lead.

interaction channel and accompanying smearing file. If a GLOBES-formatted background file labeled by the detector configuration is present in the `backgrounds` subdirectory, the background will be smeared and an additional output file created. The user is responsible for ensuring that the background events in the file correspond to the same time interval as the signal.

5.1 Water Cherenkov

Currently, two water Cherenkov configurations are provided. The LBNE detector simulation package, `WCSim`, was used to create the smearing and efficiency files for both of these.

- `wc100kt30prct`: This configuration has 100 kton of water with 30% coverage of high quantum efficiency (HQE) photomultiplier tubes. Its response is similar to that of Super-Kamiokande I (or III, IV), with 40% PMT coverage.
- `wc100kt15prct`: This configuration has 100 kton of water with 15% coverage of HQE photomultiplier tubes. Its response is similar to that of Super-Kamiokande II, with 19% PMT coverage.

For CC channels, we considered only the lepton in the final state, taking into account the energy threshold. For the NC interaction we used a simplified model of the resulting deexcitation gammas by assuming relative final energy levels according to reference [11]. Because

the reference does not provide differential final state information, we assume the distribution of these levels is independent of neutrino energy (which is an incorrect assumption, but probably not a terrible approximation). The resulting gamma cascade was simulated using relative probabilities of the transitions for a given excited state; the resulting gamma spectrum was then run through the LBNE `WCsim` detector simulation. We found rather poor efficiency for detecting these gammas, in contrast to the results in reference [18], due to the fact that gammas frequently scatter electrons below Compton threshold.

Interaction rates and smeared rates for the `wc100kt30prct` configuration and GVKM model are shown in Fig. 7. The total rates for each channel (output of `make_event_table.pl`) are shown in Tab. 1.

Channel	Events, “Livermore” model	Events, “GVKM” model
$\bar{\nu}_e + p \rightarrow e^+ + n$	27116	16210
$\nu_x + e^- \rightarrow \nu_x + e^-$	868	534
$\nu_e + {}^{16}\text{O} \rightarrow e^- + {}^{16}\text{F}$	88	378
$\bar{\nu}_e + {}^{16}\text{O} \rightarrow e^+ + {}^{16}\text{N}$	700	490
$\nu_x + {}^{16}\text{O} \rightarrow \nu_x + {}^{16}\text{O}^*$	513	124
Total	29284	17738

Table 1: Total events detected (smeared) for different models in 100 kton of water, for the `wc100kt30prct` configuration.

We expect to provide improved smearing and efficiency information for these and other water Cherenkov detector configurations as the simulation code development proceeds.

5.2 Scintillator

Currently, one scintillator configuration is provided, `scint50kt`, representing 50 kton of scintillator. The `scint50kt` smearing files were created using an assumed resolution of $\frac{\sigma}{E} = \frac{7\%}{\sqrt{E\text{MeV}}}$ from reference [19]. At the moment we assume 100% branching ratio for the 15.1 MeV gamma; however we will refine this in the near future. Efficiency is assumed to be 100%.

Channel	Events, “Livermore” model	Events, “GVKM” model
$\bar{\nu}_e + p \rightarrow e^+ + n$	17853	10617
$\nu_x + e^- \rightarrow \nu_x + e^-$	871	494
$\nu_e + {}^{12}\text{C} \rightarrow e^- + {}^{12}\text{N}$	167	447
$\bar{\nu}_e + {}^{12}\text{C} \rightarrow e^+ + {}^{12}\text{B}$	651	439
$\nu_x + {}^{12}\text{C} \rightarrow \nu_x + {}^{12}\text{C}^*$	3403	1238
Total	19601	12008

Table 2: Total events detected (smeared) for different models in 50 kton of scintillator, for the `scint50kt` configuration.

5.3 Liquid Argon

Currently one argon detector configuration is provided, `ar17kt`. For event rate estimates in liquid argon, we assume a detection threshold of 5 MeV. We assume also that suitable triggering will be provided either from charge collection or from some external trigger. The energy resolution for the smearing matrices is from Ref. [20], $\frac{\sigma}{E} = \frac{11\%}{\sqrt{E}} + 2\%$. For the CC channels in argon we have included energy deposition of the leading lepton; in the detector response, we also incorporate additional visible energy from deexcitation gammas (these gammas may also possibly help to tag the ν_e or $\bar{\nu}_e$ channels, in practice). We assume 100% efficiency, for lack of detailed efficiency information available in the literature.

Channel	Events, “Livermore” model	Events, “GKVM” model
$\nu_e + {}^{40}\text{Ar} \rightarrow e^- + {}^{40}\text{K}^*$	1138	1408
$\bar{\nu}_e + {}^{40}\text{Ar} \rightarrow e^+ + {}^{40}\text{Cl}^*$	96	66
$\nu_x + e^- \rightarrow \nu_x + e^-$	146	88
Total	1380	1562

Table 3: Total events detected (smeared) for different models in 17 kton of argon, in the `ar17kt` configuration.

5.4 Lead

Lead is a special case: for the type of detector configuration under consideration, HALO [21], electrons are practically invisible and only neutrons are observable. In practice, single and double neutron products from lead can be tagged and reconstructed; although no event-by-event energy information is available, spectral information can be inferred from the relative numbers of 1n and 2n events. The smearing files in `SNOWGLoBES` for this configuration are dummy unit matrices; efficiency of 36% for 1n channels and 56% for 2n channels is applied, although detailed reconstruction efficiencies for true 1n and 2n rates would in practice need to be applied [22]. The user is advised to make use only of interaction rates for these channels in lead and to ignore the smeared rates.

Channel	Events, “Livermore” model	Events, “GKVM” model
$\nu_e + {}^{208}\text{Pb} \rightarrow e^- + {}^{207}\text{Bi} + n$	124	173
$\nu_e + {}^{208}\text{Pb} \rightarrow e^- + {}^{206}\text{Bi} + 2n$	14	45
$\nu_x + {}^{208}\text{Pb} \rightarrow \nu_x + {}^{207}\text{Pb} + n$	53	23
$\nu_x + {}^{208}\text{Pb} \rightarrow \nu_x + {}^{206}\text{Pb} + 2n$	27	7
$\bar{\nu}_x + {}^{208}\text{Pb} \rightarrow \bar{\nu}_x + {}^{207}\text{Pb} + n$	48	19
$\bar{\nu}_x + {}^{208}\text{Pb} \rightarrow \bar{\nu}_x + {}^{206}\text{Pb} + 2n$	23	6
Total	289	272

Table 4: Total events detected for different models in 1 kton of lead, in the `halo2` configuration.

6 How to Add Your Own Stuff

It is straightforward to add new fluxes, channels, targets or detector configurations to SNOwGLoBES.

If you add new data files or configurations, the SNOwGLoBES team would appreciate if you would contact us so that the new information can be made available to all users.

6.1 Adding New Fluxes

Fluxes can be added by preparing a file according to the specifications in the GLoBES manual. The flux file must be placed in the `$SNOWGLOBES/fluxes` directory and named `fluxname.dat`, where `fluxname` is the chosen name of the flux. The file should have 501 rows with flux (or fluence) per 0.2 MeV for the different flavors in each row, for neutrino energies ranging from 0.0001 to 0.1001 GeV.

6.2 Adding New Channels

A new channel for a particular material can be added as a new row in the channels file. Each channel needs a name. Any text may be used to identify the channel, but we use a channel naming convention as follows: the channel is `neutrino_target`, where `neutrino` is the incoming neutrino flavor (`nue`, `numu`, `nutau`, `nuebar`, `numubar`, `nutaubar`). If the target is a nuclear isotope, it's written as the element abbreviation followed by the nuclear A , *e.g.* `C12`. For neutral current (NC) channels, the channel name is preceded by `nc_` (note that each incoming flavor must be listed as a separate channel, even though neutral current channels are flavor-independent). Specific exclusive final states, such as particular excitations or ejecta, can be denoted with a final tag. So for example, the charged current (CC) interaction of ν_e with ^{16}O is named `nue_160`; the NC interaction of $\bar{\nu}_\mu$ on ^{208}Pb producing double neutron final states is named `nc_numubar_Pb208_2n`. (An exception to these conventions is inverse beta decay, denoted `ibd`.)

The next item in each channel's row is the channel number; the third entry indicates whether the incoming neutrino is a neutrino (+) or an antineutrino (-); the fourth entry is the flavor of the incoming neutrino (`e`, `m`, `t`) and the final entry is the target weighting factor.

The target weighting factor requires a bit more explanation: for each material, one selects one target "reference" type, for which the weighting factor is unity. The other targets in the channels file have target weighting factors indicating the relative number of targets per reference target. For example, for water, we have chosen protons to be the reference target, and inverse beta decay has weighting factor 1. There are 0.5 ^{16}O nuclei for each proton, and 5 electrons for each proton in water, so the target weighting factors for elastic scattering on electrons are 5, and for CC and NC interactions on oxygen are 0.5.

If you add any new channels to the file, you must provide cross-sections for these channels and put them in the `$SNOWGLOBES/xscns` directory. The cross-section files must be prepared according to the specification in the GLoBES manual, and must be named `xs_channelname.dat`. The cross section should be provided between 0.0005 and 0.100 GeV.

6.3 Adding New Detector Configurations

The `detector_configurations.dat` file contains a list of available detector configurations. The first entry in each row is the detector configuration name. The second entry is the mass in kilotons. The third entry is a target normalization factor: this is reference targets (see section 6.2) per amu in the detector configuration material. For example, for water (18 amu per molecule), for which the reference target is protons, the target normalization factor is 2/18. For lead, the reference target is ^{208}Pb ; the target normalization factor is 1/208.

Each new detector configuration must have smearing and (optionally) efficiency files associated with it for each channel the user wishes to calculate rates for. The smearing and post-smearing efficiency files must be prepared according to the specifications in the GLOBES manual. SNOwGLOBES uses 200 true energy bins from 0.0005 to 0.100 GeV and 200 sampling bins over the same range. Smearing files must go in the `$$SNOWGLOBES/smear` directory and be named as follows: `smear_channelname_detconfigname.dat`. Efficiency files must go in the `$$SNOWGLOBES/effic` directory and be named as follows: `effic_channelname_detconfigname.dat`. If the post-smearing efficiency file is absent, then 100% post-smearing efficiency is assumed.

6.4 Adding A New Detector Material

To add an entirely new detector material, one would create a new channels file with interaction channels for that material, along with appropriate cross-section files (and a detector configuration employing that material).

6.5 Adding A New Background

The background calculated by SNOwGLOBES is presumed to be the sum of all relevant backgrounds in the appropriate time interval, as provided by the user. Backgrounds can be added by creating a file in the `backgrounds` subdirectory, `bg_chan_detconfigname.dat`. If no file is present in this directory for a given detector configuration, SNOwGLOBES will ignore the background. An accompanying smearing file must be provided by the user, `$$SNOWGLOBES/smear/smear_channelname_detconfigname.dat`. If the background is already smeared, this can be the unit matrix.

7 Future Upgrades

There are a number of future upgrades on our to-do list:

- Inclusion of more targets, channels and fluxes.
- Currently, SNOwGLOBES can handle detected energies in the 0.5-100 MeV range only. We plan an upgrade to allow modified output energy ranges, which will allow inclusion of channels for which the appropriate smeared energy range is different, such as coherent elastic scattering on protons or nuclei.

- As knowledge of detector responses improves (for instance as detector simulation codes improve, and measurements are made) we will update the smearing matrices accordingly.
- Computation of angular distributions for channels with asymmetries.
- Inclusion of additional cross-sections to allow evaluation of cross-section-related uncertainties.
- Addition of frameworks for treatment of time-dependent fluxes, and for treating experimental and theoretical uncertainties.
- Expansion of capability to include multiple, distinct backgrounds.
- Inclusion of non-supernova fluxes, *e.g.* stopped-pion fluxes.

Bug reports, suggestions and contributions are very welcome. Please contact Kate Scholberg at `schol@phy.duke.edu`.

8 Acknowledgements

This work was initiated in the context of the Supernova Burst Physics Topical Group of the Long Baseline Neutrino Experiment collaboration, for which research activities are primarily supported by the U.S. Department of Energy and the National Science Foundation. AB and NK were supported for work at Duke University by the Deutscher Akademischer Austausch Dienst summer internship program. The authors wish to thank the members of the Physics Working Group of the LBNE collaboration, and the Institute for Nuclear Theory at the University of Washington for its hospitality during the summer of 2010.

A Change log

- Version 1.0 is the initial release.
- Version 1.1: the target weighting factors are applied automatically by `supernova.pl`, which creates correctly-weighted output event rate files from the raw unweighted files (the latter now designated `_unweighted.dat`). Example plotting and event table scripts now no longer apply the weighting factor to event rates, and the user is no longer responsible for doing it.
- Version 1.2: capacity for handling backgrounds is added; a single background rate per detector configuration is enabled, if provided by the user. A default background for the `ar17kt` configuration is included.

B GPL

GPL documentation blurb goes here

References

- [1] Amol Dighe. Physics potential of future supernova neutrino observations. *J. Phys. Conf. Ser.*, 136:022041, 2008.
- [2] Kate Scholberg. Supernova neutrino detection. 2007.
- [3] Patrick Huber, M. Lindner, and W. Winter. Simulation of long-baseline neutrino oscillation experiments with GLOBES. *Comput. Phys. Commun.*, 167:195, 2005.
- [4] <http://www.mpi-hd.mpg.de/lin/globes/>.
- [5] M. Bass et al. A Study of the Physics Potential of the Long-Baseline Neutrino Experiment Project with an Extensive Set of Beam, Near Detector and Far Detector Configurations. 2010.
- [6] <http://root.cern.ch/drupal/>.
- [7] T. Totani, K. Sato, H. E. Dalhed, and J. R. Wilson. Future detection of supernova neutrino burst and explosion mechanism. *Astrophys. J.*, 496:216–225, 1998.
- [8] Jerome Gava, James Kneller, Cristina Volpe, and G. C. McLaughlin. A dynamical collective calculation of supernova neutrino signals. *Phys. Rev. Lett.*, 103:071101, 2009.
- [9] Alessandro Strumia and Francesco Vissani. Precise quasielastic neutrino nucleon cross section. *Phys. Lett.*, B564:42–54, 2003.
- [10] William J. Marciano and Zohreh Parsa. Neutrino-Electron Scattering Theory. *J. Phys.*, G29:2629–2645, 2003.
- [11] E. Kolbe, K. Langanke, and P. Vogel. Estimates of weak and electromagnetic nuclear decay signatures for neutrino reactions in Super-Kamiokande. *Phys. Rev.*, D66:013007, 2002.
- [12] E. Kolbe, K. Langanke, and P. Vogel. Weak reactions on ^{12}C within the Continuum Random Phase Approximation with partial occupancies. *Nucl. Phys.*, A652:91–100, 1999.
- [13] B. Armbruster et al. Measurement of the weak neutral current excitation $C-^{12}(\nu(\mu)\nu'(\mu))C^*-^{12}(1+,1,15.1\text{-MeV})$ at $E(\nu(\mu)) = 29.8\text{-MeV}$. *Phys. Lett.*, B423:15–20, 1998.
- [14] Ines Gil Botella and A. Rubbia. Decoupling supernova and neutrino oscillation physics with LAr TPC detectors. *JCAP*, 0408:001, 2004.
- [15] E. Kolbe, K. Langanke, G. Martinez-Pinedo, and P. Vogel. Neutrino nucleus reactions and nuclear structure. *J. Phys.*, G29:2569–2596, 2003.
- [16] J. Engel, G. C. McLaughlin, and C. Volpe. What can be learned with a lead-based supernova-neutrino detector? *Phys. Rev.*, D67:013005, 2003.

- [17] N. Paar, T. Suzuki, M. Honma, T. Marketin, and D. Vretenar. Uncertainties in modeling low-energy neutrino induced reactions on iron group nuclei. 2011.
- [18] K. Langanke, P. Vogel, and E. Kolbe. Signal for supernova ν_μ and ν_τ neutrinos in water Čerenkov detectors. *Phys. Rev. Lett.*, 76:2629–2632, 1996.
- [19] K. Eguchi et al. First results from KamLAND: Evidence for reactor anti- neutrino disappearance. *Phys. Rev. Lett.*, 90:021802, 2003.
- [20] S. Amoruso et al. Measurement of the mu decay spectrum with the ICARUS liquid argon TPC. *Eur. Phys. J.*, C33:233–241, 2004.
- [21] C. A. Duba et al. HALO: The helium and lead observatory for supernova neutrinos. *J. Phys. Conf. Ser.*, 136:042077, 2008.
- [22] HALO collaboration. In preparation.

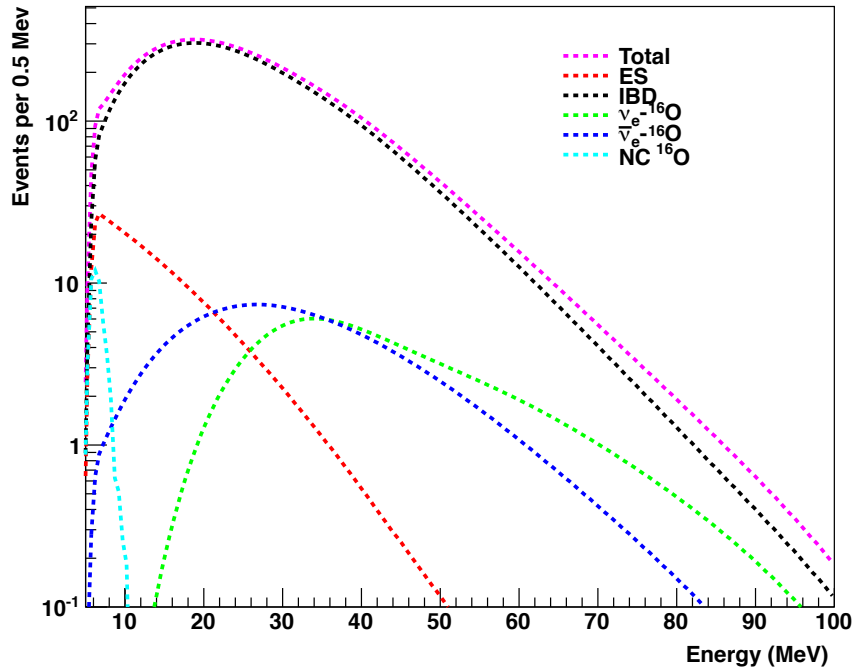
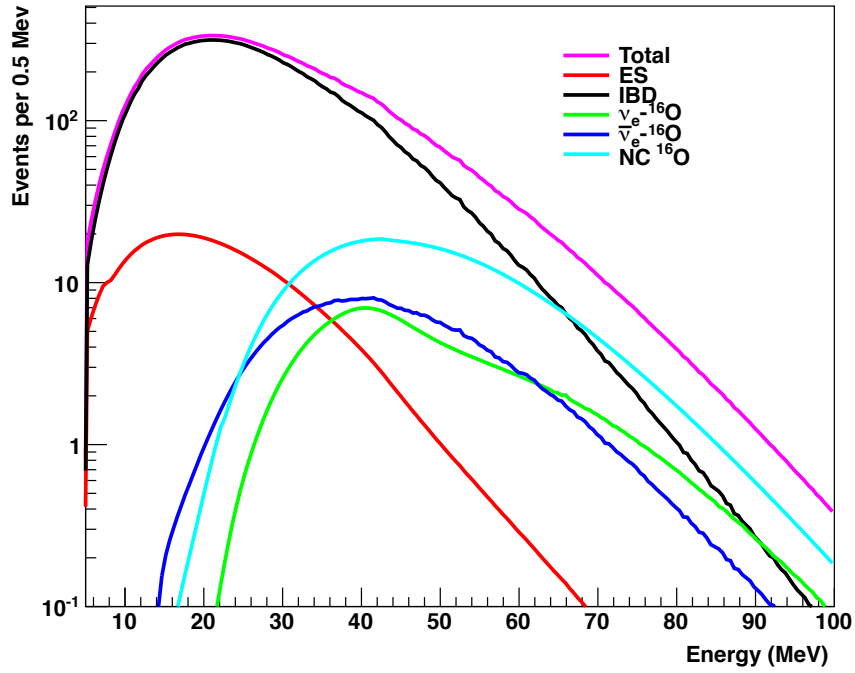


Figure 7: Event rates in 100 kton of water, for the GVKM model and 30% PMT coverage (events per 0.5 MeV). Top: interaction rates as a function of true neutrino energy; bottom: "smeared" rates as a function of detected energy.

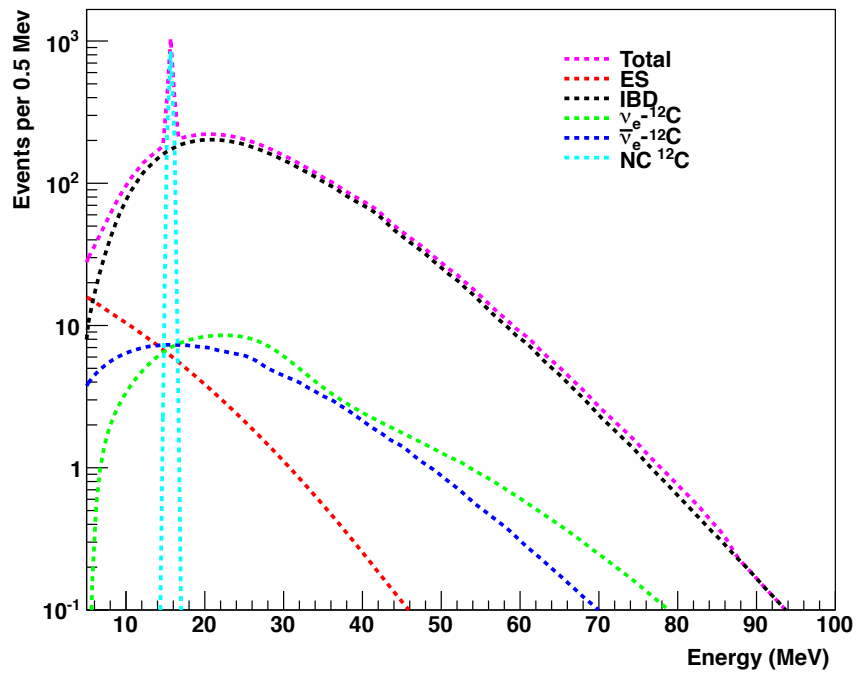
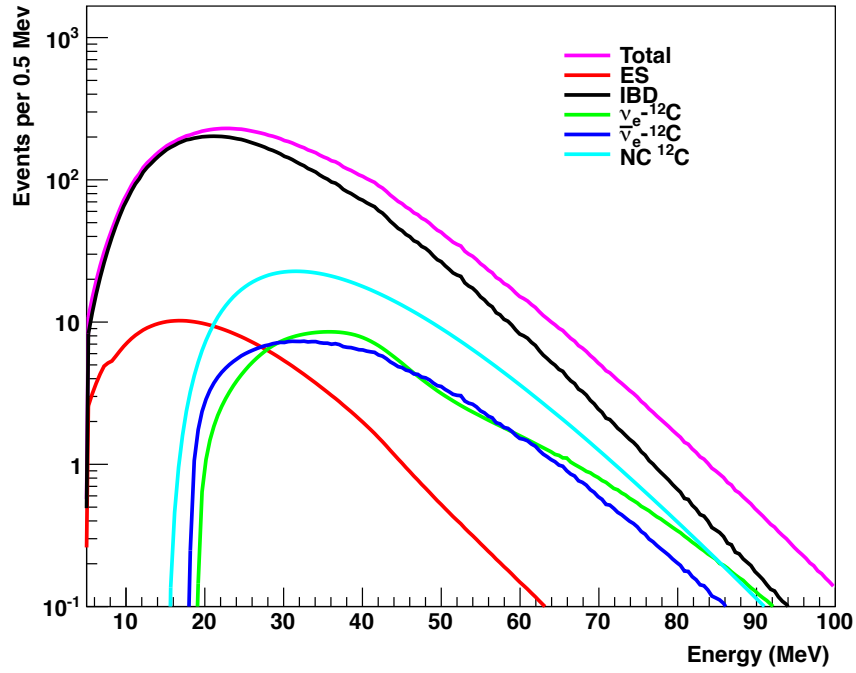


Figure 8: Event rates in 50 kton of scintillator, for the GVKM model (events per 0.5 MeV). Top: interaction rates as a function of true neutrino energy; bottom: "smearred" rates as a function of detected energy.

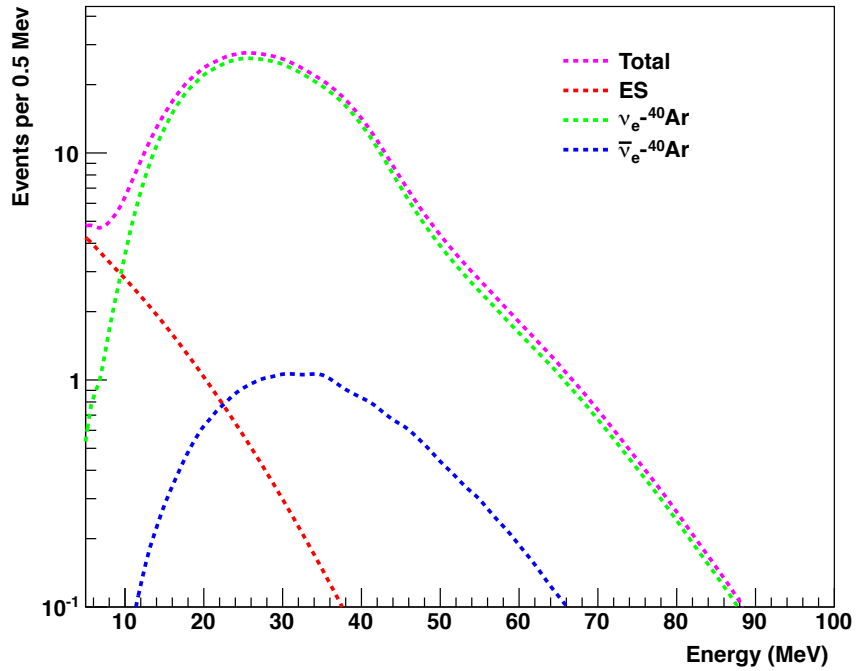
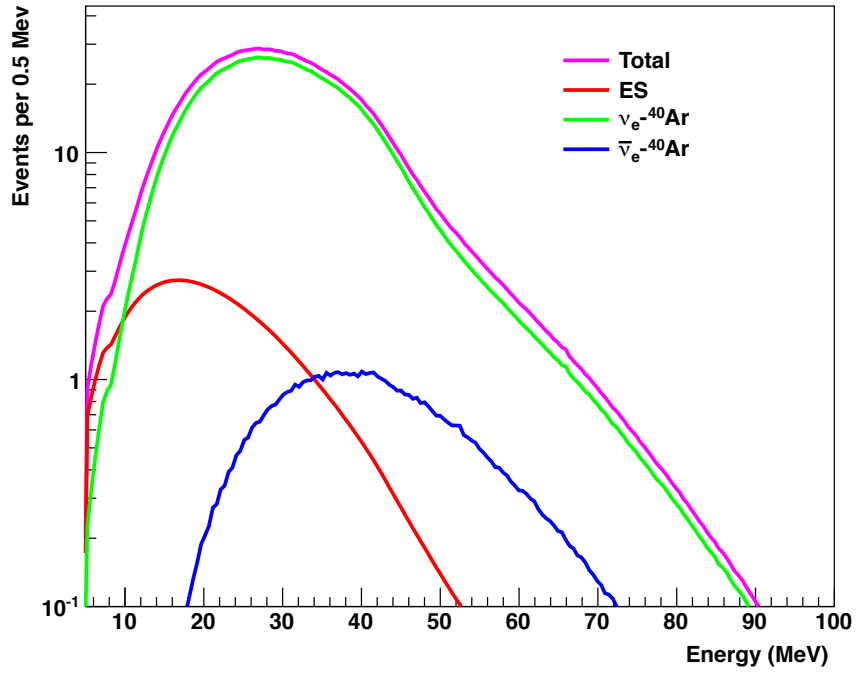


Figure 9: Event rates in argon, for the GVKM model (events per 0.5 MeV). Top: interaction rates as a function of true neutrino energy; bottom: “smearred” rates as a function of detected energy.

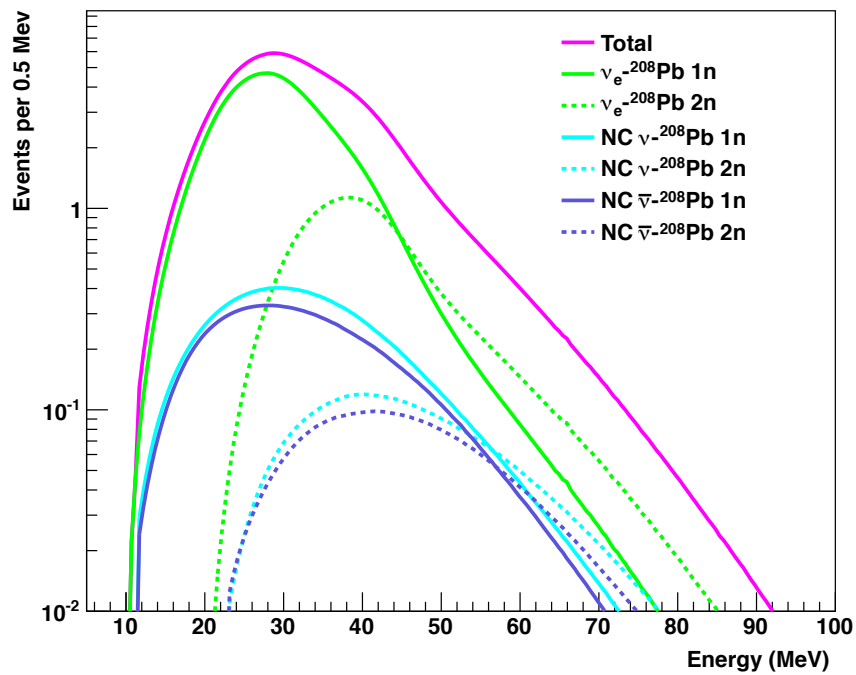


Figure 10: Event rates in 1 kton of lead (events per 0.5 MeV) for the GVKM model. These are interaction rates as a function of true neutrino energy.